PERFORMANCE ASSESSMENT TOOL FOR AUV BASED MINE HUNTING

Øivind Midtgaard Norwegian Defence Research Establishment (FFI), Kjeller, Norway
Ivar Alm Norwegian Defence Research Establishment (FFI), Kjeller, Norway
Torstein O Sæbø Norwegian Defence Research Establishment (FFI), Kjeller, Norway
Marc Geilhufe Norwegian Defence Research Establishment (FFI), Kjeller, Norway
Roy E Hansen Norwegian Defence Research Establishment (FFI), Kjeller, Norway

Email: Oivind.Midtgaard@ffi.no

1 INTRODUCTION

Autonomous Underwater Vehicles (AUVs) have become an essential asset in naval mine hunting, due to their superior sensor data quality, efficiency, covertness and reduction in risk to personnel. The first phase of these operations typically consists of an AUV survey to collect high-resolution, side-looking sonar imagery of the complete area. The images are analysed by a human operator or Automatic Target Recognition (ATR) system[1] to detect, classify and geo-reference all contacts (mine-like sonar responses). In a second phase, contacts are selected based on the resulting contact map and the operation objectives, and sequentially reacquired to perform identification and neutralisation (if confirmed mine). Neutralisation currently involves a surface vessel, as it requires a diver or Remotely Operated Vehicle (ROV) to deposit an explosive charge by the mine. Identification imagery can alternatively be obtained by an AUV equipped with camera[2].

Reliable performance estimates are imperative for both planning and evaluation of Mine Counter Measures (MCM) operations. Too pessimistic estimates make the operation consume unnecessary time and resources, while too optimistic estimates may result in unacceptable ship losses. The total performance is given as Percentage Clearance (PC), i.e. the fraction of mines successfully eliminated from the area, or the remaining risk for transiting vessels. The total performance depends on the success rates from all steps in the mine hunting operation. Of particular importance is the survey effectiveness, which can be quantified by the probability of correctly detecting and classifying mines (P_{dc}), together with the associated false alarm rate (non-mine contacts). This performance depends on the environment, mine type and complete survey system (including sensor, platform, sensing configuration, data processing and data analysis system). The littoral environment varies significantly in space and time, and affects the performance through many factors: seafloor type, water depth, sea state, seafloor roughness, currents, clutter density, etc. Complete and accurate environmental information is rarely available prior to a mine hunting operation and predictions may be uncertain. *In situ* sensor data is thus required for post-mission assessment of the performance actually achieved, as well as for in-mission adaptation of the AUV plan to obtain the aimed performance. In the literature, this is also referred to as through-the-sensor[3] and data-driven[4] performance estimation.

Some mine hunting performance models are tailored for specific sensor systems. As an example, data from the AQS-20 side-looking and volume sonars have been used to estimate bottom roughness, clutter density and probability of mine burial in the local environment[3]. This provides the doctrinal bottom type and the performance through table look-up. A few generic approaches, relying only on side-looking sonar imagery, are described more detailed below.

One approach[5] blends modelled targets into the recorded sonar imagery and applies ATR to estimate the achieved P_{dc}. First, the beam pattern, reflectivity and height maps are estimated from the sonar image through an iterated inversion process. 3D mine models are used to insert targets by altering the local bathymetry and reflectivity. Sonar simulation then produces an augmented image incorporating target-background interactions due to seafloor slope and occlusions. A texture

classification module segments the seafloor into three classes: smooth, rippled and complex (i.e. rocks, sea grass). Finally, comparison of injected target positions with ATR results yields P_{dc} as function of seafloor class, mine type and range. A closely related approach[4] avoids the calculation-intensive sonar inversion by inserting target signatures through ray-tracing combined with modelled contrast values for target echo and shadow relative the local background level.

Another general approach[6] estimates the probabilities for mine detection and classification (P_d and P_c) separately and combines them in a final stage: $P_{dc} = P_d * P_c$. The two main factors affecting P_d are assumed to be reverberation (sea bottom and sea surface) and lack of target insonification due to occlusion or burial. The influence from reverberation and occlusion is estimated through the latent parameters shadow-to-background contrast and bottom roughness, respectively. Further, P_c is assumed to depend on four parameters that can be combined into an effective Signal-to-Noise Ratio (SNR). The first parameter is sonar SNR, estimated as the maximum pixel value divided by the mean value within a sliding window. The next two parameters are related to average target echo length and area, measured in image pixels. The fourth parameter is the shape parameter of the statistical K-distribution, estimated from pixel values within a small sliding window. The mappings (interrelation) between these parameters and P_c / P_d are determined offline by applying ATR on a large and varied set of synthetic sonar images, extending the full parameter space. For performance estimation, the variable parameters may then be either predicted via the model combined with user input of sonar type and bottom roughness (for planning), or estimated from *in situ* data (for evaluation).

This paper presents a performance assessment model that is an extension of our earlier work[7-9]. It is related to [6], but uses different latent parameters for performance mapping. The model is developed for mine search with state-of-the-art sonars such as Kongsberg's HISAS 1030[10], but is generic as it also applies to other side-looking sonar systems with real or synthetic apertures. The calculation of parameter values from sensor data is sensor dependent, though. The idea is to utilize the additional information provided by advanced sensors to achieve more accurate estimates, while still supporting low-end sensors.

Section 2 presents our performance model. The two main *in situ* parameters, image quality and image complexity, are described in Sections 3 and 4, respectively. Section 5 describes the implementation of the model into a prototype tool and shows some results with real sonar data. Section 6 summaries the paper and outlines some future work.

2 PERFORMANCE MODEL

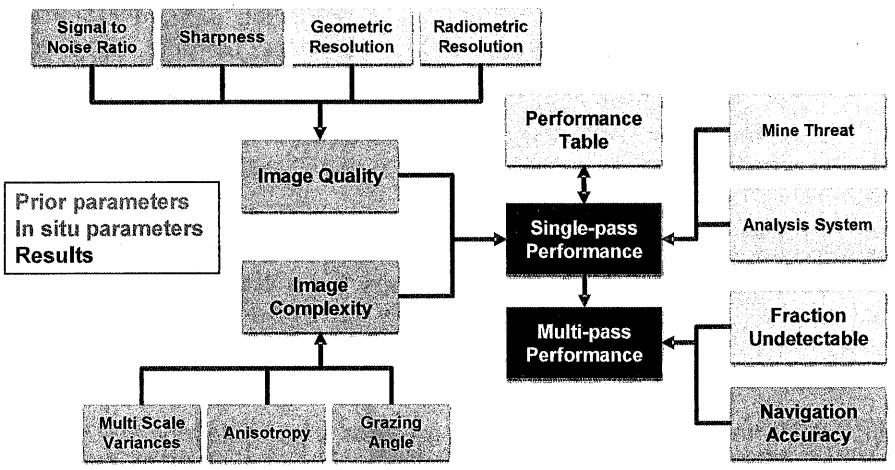

Figure 1: Proposed performance assessment model for AUV based mine hunting.

Figure 1 shows the data flow in our model for estimating the performance P_{dc}. The light blue boxes are parameters calculated from local sensor data, while the yellow boxes are *a priori* parameters. The model has two main *in situ* parameters, that both attain normalized values between zero and one. Firstly, the image quality estimates how well a potential proud seafloor mine will be represented in the sonar image, i.e. whether the spatial resolution and intensity contrast allow reliable target recognition. Quality is calculated from four sub-parameters, as described in Section 3. Secondly, the image complexity estimates how difficult it is to recognize a potential mine in the given image, as P_{dc} is degraded by background responses that resemble or interfere with target highlight or shadow. Complexity is calculated from three sub-parameters, as described in Section 4.

The performance table in Figure 1 contains calibrated performance values for all combinations of image quality and image complexity values, typically given as Receiver Operating Characteristic (ROC) curves with corresponding figures for P_{dc} and false alarm rate. The table is created offline for a specified mine threat and data analysis system using an extensive database of sonar imagery from simulations or sea trials with mine ground truth.

The mine threat indicates the expected mine types in the area, and is assumed known from MCM operation intelligence. The mine threat has a significant impact on P_{dc} as modern stealth mines are more difficult to classify than traditional cylinder mines. Although not indicated in Figure 1, both image quality and image complexity depend on typical target dimensions, i.e. mine threat. The data analysis system can be a human operator or a specified ATR system. This is an important parameter as current ATR systems typically perform worse than a skilled human, at least for challenging scenarios. Also, performance varies between operators with different levels of expertise and alertness.

The final prior parameter is the fraction of undetectable mines due to burial. Mines may become buried during seafloor impact (in soft sediments or dense vegetation) or by sediment movement over time (scouring, slides, etc.). The probability of mine burial should preferably have been measured *in situ*, but as it cannot be inferred from current side-looking sonar imagery alone, we consider it to be an *a priori* input parameter. The fraction of undetectable mines does not include missed mines due to occlusions, i.e. seafloor roughness. Occluded areas will have low SNR values (and thus low image quality) in the shadow centres and high complexity values along the perimeters.

The performance for a survey is calculated through a two-step evaluation processing. First, single pass performance values are generated from table look-ups based on *in situ* estimates of image quality and complexity from each sonar view of a seafloor patch. The single pass values are mapped into a geo-referenced grid and overlapping data are fused into a multi-pass performance map of P_{dc}. The fraction of undetectable (buried) mines is used to downscale the performance, while the reported navigation accuracy is used for data smoothing during multi-pass fusion.

The detection and classification performance, P_{dc}, is only a subset of the total MCM performance measure, PC. Estimation of PC also requires consideration of the probabilities for successful contact re-acquisition, identification and neutralisation. If these four tasks are assumed to be statistically independent, PC can be estimated as the product of their individual probabilities. The probability for contact re-acquisition depends on the relative navigation accuracy and clutter density. The identification probability varies with image contrast (visibility) and object surface condition (biofouling, corrosion).

3 IMAGE QUALITY

We define the image quality (see Figure 1) as the product of four metrics: theoretical geometric resolution, sharpness, radiometric resolution and signal-to-noise ratio. All of the four metrics are mapped to a value between zero and one using the Sigmoid function, thus the image quality also becomes a value between zero (low quality) and one (high quality).

The true geometric resolution is typically defined as the minimum distance between two reflectors that can be resolved in the image. In the range dimension, the theoretical resolution is given by the bandwidth. In the along-track dimension the theoretical resolution is given by the element size for Synthetic Aperture Sonar (SAS)[11], and by the product of the angular resolution and the range for real aperture sonar. The achieved geometric resolution is also dependent on the SNR and navigation accuracy[12]. We have chosen to separate the true geometric resolution into two variables: theoretical resolution and sharpness. The general idea is that the theoretical resolution is treated as a SAS system constant (a range dependent parameter for real aperture sonar systems), while sharpness varies. When the geometric resolution is mapped to a quality metric, the target size is also used as an input parameter since it is the number of independent pixels on the target which affects the classification performance, and not the absolute resolution.

We use the term sharpness as in the meaning of how close the true image resolution is to the theoretical resolution. A perfectly sharp image (sharpness = 1) has theoretical resolution and no image artefacts. In SAS, defocus (mostly caused by random navigation errors)[13] and grating lobes (mostly causes by periodic navigation errors)[14] are common. For a real aperture sonar system, artefacts caused by nonlinear platform motion are frequent. Ideally, the sharpness should be estimated directly from the sonar image, but since there is no established way of doing that, we suggest estimating the sharpness from metadata. To achieve a physical meaning of the sharpness parameter we define sharpness such that:

$$\textit{True resolution} = \textit{Theoretical resolution} / \textit{sharpness} \qquad (1)$$

where $0 \leq \textit{sharpness} \leq 1$. In [8] we discuss how to construct the sharpness from the metadata for SAS systems. Most important are the navigation accuracy, the sound speed accuracy and the out-of-plane deviations in relation with bathymetric errors (errors in the imaging geometry).

The radiometric resolution is the accuracy of the estimated value in each pixel. To accurately estimate the radiometric resolution the sonar has to be fully calibrated energy wise. Most imaging sonar systems are not calibrated, but the use of absolute target strength is common in radar[15] and increasingly important also in sonar[16]. Sonar images also have to be despeckled[15] to avoid an artificial low radiometric resolution. In addition, the use of too few bits per sample will lead to intensity saturation which affects the radiometric resolution.

The signal-to-noise ratio in a sonar image can be estimated from the sonar coherence. For an interferometric sonar, the interferometric coherence, i.e. the similarity between the signals on the different receiver arrays, is the natural metric[7;17]. For a non-interferometric system, the temporal coherence in micro-navigation, i.e. the similarity between signals from succeeding pings, can be used instead[18]. The most dominant noise source when the sonar is operated in shallow areas is surface multipath[19]. Figure 2 shows SAS images and corresponding coherences for two different example scenes. Notice the strong dependence between low coherence and low image quality.

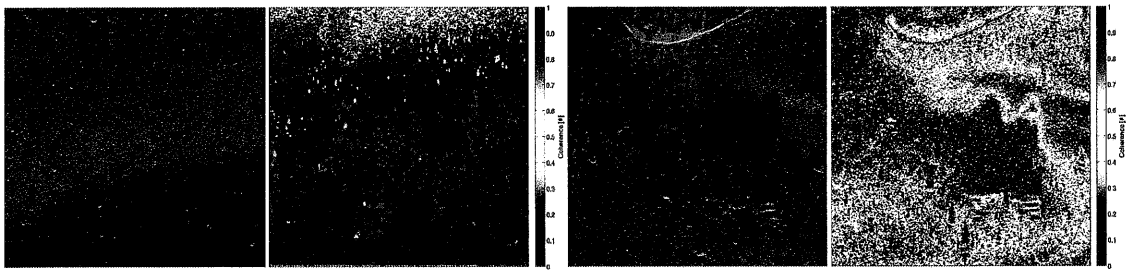

Figure 2: SAS image with corresponding interferometric coherence for a 50x50m area with high image quality (two leftmost panels), and for a 50x50m area with low image quality (two rightmost panels).

4 IMAGE COMPLEXITY

The image complexity parameter (see Figure 1) is a function of three sub-parameters: multi-scale variances, anisotropy and grazing angle. All four parameters are continuous measures bounded between zero and one. The complexity quantifies the degree of image texture caused by e.g. seafloor roughness, clutter and reverberation level gradients. Large values indicate regions where mine hunting is difficult due to intensity variations over mine-sized scales, while small values indicate benign, homogeneous regions. This continuous characterisation is fundamentally different from image segmentation into distinct regions of different seafloor types[5], even though both approaches are based on image texture descriptors. The multi-scale variances parameter is related to the seafloor complexity parameter in [20].

We refer to the complexity as a characteristic of the image and not the seafloor, to emphasize that the sonar image is a function of not merely the seafloor features, but also sensing geometry, sensor hardware, data processing, sonar conditions and water column characteristics. For instance, the image texture caused by sand ripples is dependent on aspect angle, grazing angle and sonar frequency. Also, water column fluctuations may induce wavy intensity patterns on smooth seafloors[21].

Our method[9] for calculating image complexity uses wavelet variances obtained from the coefficients of the Maximal Overlap Discrete Wavelet Transform (MODWT)[22;23], which is non-subsampled and shift-invariant. It is well suited for scale-based analysis of image texture, and allows us to focus on intensity variations over mine-size scales. Combining one dimensional wavelet (i.e., differencing) and scaling (i.e., averaging) filters into two dimensions yields three types of directional coefficients capturing horizontal, vertical and diagonal structures. The multi-scale variances parameter is estimated by first adding the three directional wavelet variances from small windows at each scale and then calculating the weighted sum of these values over the appropriate scale interval.

The image complexity measure should take into account that mine hunting is more difficult on seafloors with random clutter (e.g. rocks) than well-structured, oriented texture (e.g. sand ripples) even if the intensity variances may be similar. We thus determine anisotropy, i.e. the presence of directionality in the image, by ratios of the local horizontal and vertical wavelet variance of relevant scales and 45° rotated versions thereof. It is used to subdue the influence of ripple regions in the complexity measure without disturbing randomly oriented seafloor regions (see Figure 3).

The sonar grazing angle affects both intensity variances and P_{dc} performance. For steep angles, object shadows become too short to reveal significant shape information and object echoes have less contrast to the surrounding seafloor as their incident angles are fairly similar. For small angles, the shapes of the elongated object shadows are sensitive to even minute variations in seafloor slope. The third sub-parameter incorporates this behaviour by increasing the complexity measure for unfavourable grazing angles.

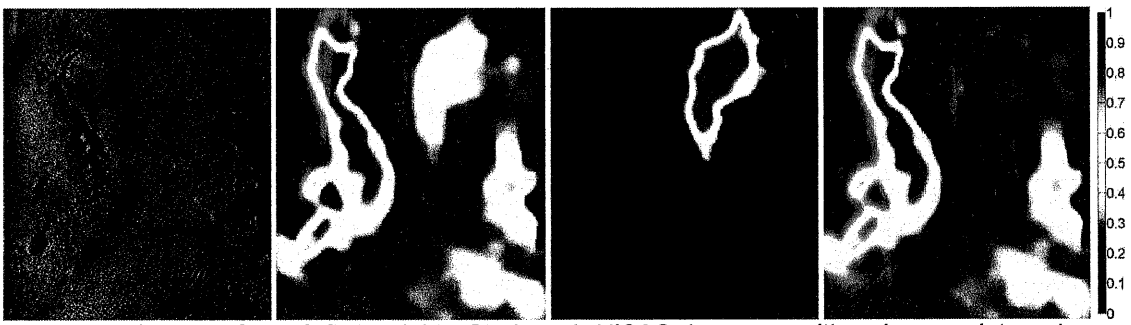

Figure 3: Images from left to right: Starboard HISAS image, multi-scale wavelet variance, anisotropy and image complexity. The images cover 19-114m across-track and 113m along-track. The area of high anisotropy values is due to sand ripples in the SAS image.

5 IMPLEMENTATION AND EXAMPLE RESULTS

We have implemented our performance model as a prototype C++ tool named *MCM Insite*. The tool reads image quality and image complexity data from an AUV mission, processes the data into a geo-referenced grid and creates single-pass performance maps based on table look-ups. A multi-pass performance map is then generated by fusing results from overlapping survey lines, assuming statistical independence (i.e. different sensing geometry). *MCM Insite* can be used with different sonar systems, as the sensor specific calculations of image quality and image complexity are performed outside the tool. We have implemented methods for HISAS 1030 as described in Sections 3 and 4. The parameters geometric and radiometric resolutions are both set to 1.0. For typical mines with a smallest dimension 0.5m, the nominal resolution of HISAS[2] yields at least around 15 independent along-track pixels on the object, which is compatible with reliable classification[24]. The parameters grazing angle and fraction undetectable mines are not yet implemented.

The tool has a graphical user interface to select settings (including grid cell size) and visualize the result maps. It can also export results in file formats supported by standard Geographic Information Systems (GIS), e.g. ArcGIS or Global Mapper. Currently, we have implemented the formats GeoTIFF and PNG with world file. Although the prototype tool is intended for post-mission analysis, the performance model's computational requirements permit in-mission processing within an AUV.

A performance table is specific for the mine threat and analysis system. It is generated by testing the analysis system's ability to detect and classify mines in sonar images of varying quality and complexity. A large set of sonar data with ground truth targets is needed for this calibration. We prefer real data over simulated data to ensure validity. The performance tables are stored as text files outside the tool.

MCM Insite produces single-pass and multi-pass geographical maps of not only the performance P_{dc}, but also the *in situ* parameters image quality and image complexity, as well as their sub-parameters SNR, sharpness and anisotropy. This may seem illogical, as these parameters depend on e.g. sensing geometry, and are not solely a function of global position. We have found, however, that these maps are useful to understand the underlying reasons for instances of degraded performance. In an operational setting, this may be valuable information in order to decide if and where additional survey lines should be planned. Unlike performance, the single-pass data for these parameters are currently fused by taking the maximum value of each grid cell. If depth measurements are available, *MCM Insite* also generates a bathymetry map using the same grid.

The tool is demonstrated on a data set recorded with HISAS mounted on FFI's HUGIN-HUS AUV during the MANEX'13 trials[25], which were arranged by the NATO Science and Technology Organisation Centre for Maritime Research and Experimentation (CMRE) in autumn 2013. Figure 4 shows a sonar mosaic from the survey of a bay on the southern coast of Elba Island, Italy. The water depth in the displayed area varied between 5 and 55 m. The mosaic reveals varying seafloor conditions, where the large, bright region in the upper part is sea grass (*Posidonia oceanica*) and the large, darker area below is smooth sediments. The sea grass becomes sparse in the shallowest region (northern edge), thereby exposing patches of sediments. While entering the survey rectangle from south-west, the AUV passed a mixed area with seafloor clutter, roughness and rock outcrops. The dark, almost horizontal stripes are due to decreased intensity close to the sonar blind zones.

Figure 5 presents corresponding multi-pass maps generated by *MCM Insite*. The first map shows the bathymetry with the survey lines overlaid. The second map shows the image quality, where red and yellow colours indicate regions of poor quality in the shallowest region (upper map edge) and along the entry track. Inspection of the maps for the sub-parameters coherence and sharpness (not shown) reveals that this is due to low coherence, probably caused by surface multipath and rock outcrop shadows, respectively. The quality is elsewhere good, although it degrades somewhat at the map perimeter and for depths smaller than 30m.

The third map in Figure 5 shows image complexity, where values are low for the smooth sediments and high for the rock outcrops and clutter. Also, the transition zones between bright sea grass and dark sediments yield increased complexity. Note that complexity is not calculated in regions of low coherence values. The areas fully covered by sea grass show little texture in the sonar mosaic and give fairly low complexity values (larger than the sediments, though). One could argue that these areas should be characterised as highly complex because mine hunting will be difficult. This is, however, due to mines becoming buried in the vegetation and not due to background intensity patterns. Other parameters (i.e. fraction of undetectable mines) address this issue in our performance model.

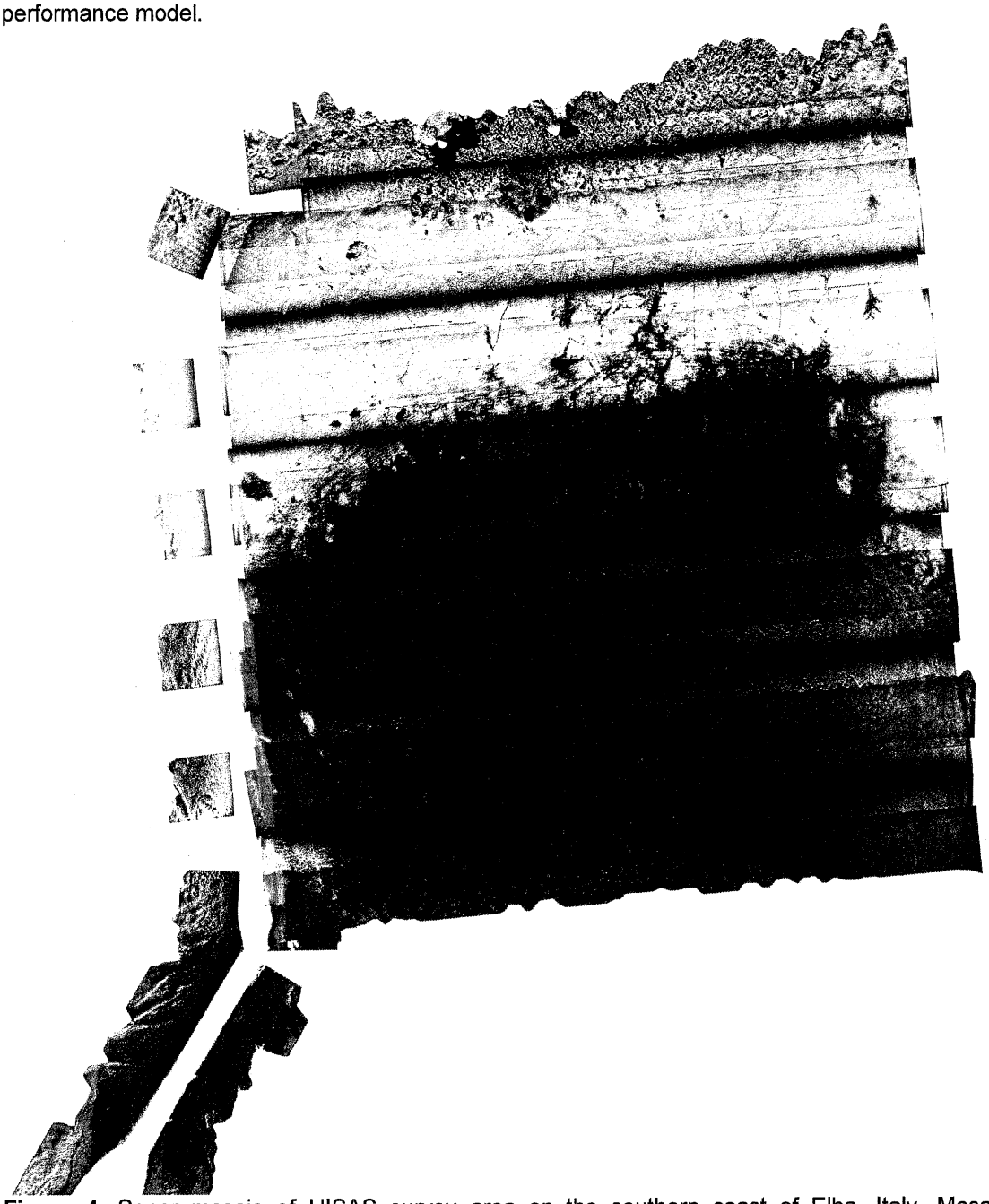

Figure 4: Sonar mosaic of HISAS survey area on the southern coast of Elba, Italy. Mosaic magnitude is calculated as magnitude mean of all SAS pixels within each 25x25 cm grid cell. The main rectangular area covers approximately 1.5x1.7 km.

The fourth map in Figure 5 shows the estimated performance, P_{dc}. The dedicated colour table segments the performance into three levels, based on user selectable threshold values. The idea is to provide the user with an overview of where the desired performance has been achieved, where some more survey efforts are required and where the current performance is poor. We see that P_{dc} > 80% has been achieved for most of the survey area, except close to the shore and for the entry track in south-west. In both cases, a combination of low quality (low coherence) and high complexity limits performance. There are some yellow segments in the upper part of the survey rectangle, though. These locations correspond to slightly reduced quality upon the survey lines, where the seafloor is only imaged once (at far range on the adjacent line). Additionally, the complexity is somewhat higher than in the lower part of the rectangle.

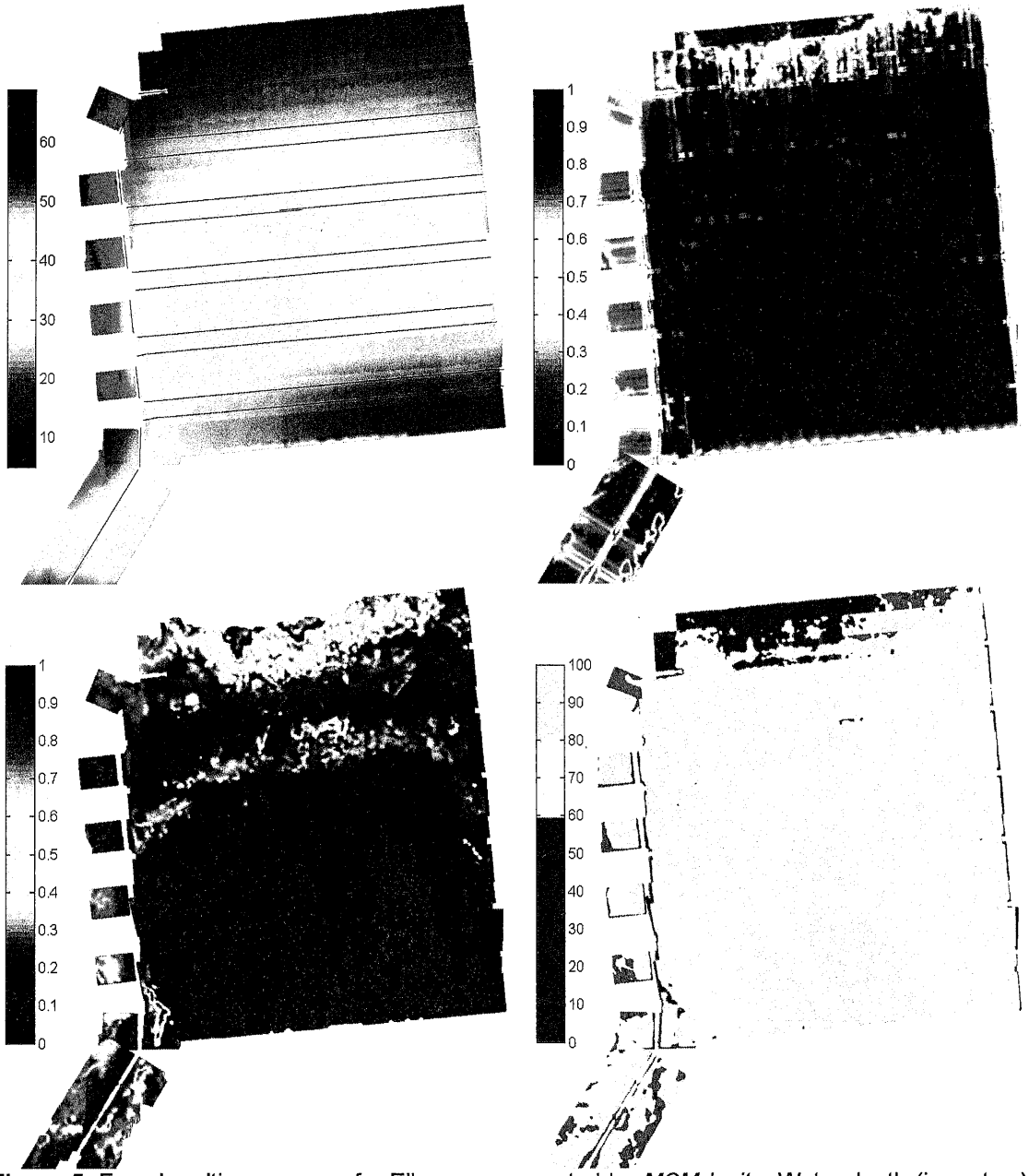

Figure 5: Fused multi-pass maps for Elba survey created by *MCM Insite*: Water depth (in meters) with vehicle tracks overlay (top left), image quality (top right), image complexity (bottom left) and estimated P_{dc} performance (bottom right).

The P_{dc} map in Figure 5 is created to illustrate our performance model and the available outputs from *MCM Insite*. It does not necessarily reflect the actual mine hunting capabilities of the HISAS system, for several reasons. Firstly, an uncalibrated, performance table has been used to produce results that are not military classified. Secondly, the parameter for mine burial potential is not yet implemented in the tool, and performance estimates may thus be inaccurate within the field of sea grass.

6 SUMMARY AND FUTURE WORK

This paper presents a model for performance assessment of mine hunting operations where AUVs equipped with side-looking sonar are used to survey the seafloor of an area. The model contains two main parameters, image quality and image complexity, that both depend on the underwater environment. The image quality quantifies how well a seafloor mine will be represented in the sonar image, while the image complexity quantifies how difficult it will be to recognize a mine against the image background. For post-mission evaluation, these parameters are estimated locally from the actual sonar data. For pre-mission planning, simulations and/or historical data can be used instead, but the resulting estimates will be less reliable. The performance is determined from a prior mapping between the two parameters and the probability for mine detection and classification.

We have implemented the model into a prototype C++ evaluation tool named *MCM Insite*. The tool reads image quality and complexity values from files, and generates a geographical performance map by fusing results from all survey lines. This performance map can be used to optimise further mine hunting efforts and select the safest transit route through the area. The calculation of image quality and complexity is sensor model specific, and thus lies outside the generic tool. The concept is to utilize additional data provided by advanced sensors to achieve more accurate estimates, while still supporting low-end sensors. FFI has implemented calculation methods for HISAS 1030, and is currently generating a corresponding performance mapping using a large database of real sonar data with target ground truth. We will evaluate the performance tool on SAS data from sea trials in varied environments.

The current *MCM Insite* a stand-alone program intended for post-mission processing. We will refine the tool and transfer it to the Royal Norwegian Navy (RNoN) for operational use with the latest version of the HUGIN AUVs that are currently under acquisition in Norway. We will also make a modified version for delayed real-time processing within the AUV to enable autonomous mission adaptation using achieved performance.

MCM Insite is owned by FFI and the RNoN and is not intended to be a commercial product. The aim is to distribute the tool within NATO on a government to government basis. We are seeking cooperation with relevant research institutions to evaluate and further develop the model and tool, including support for other sonar models (real and synthetic apertures).

7 REFERENCES

1. J. Stack. *Automation for underwater mine recognition: current trends and future strategy*. Proc.of SPIE. Vol. 8017. Orlando, FL, USA. (May 2011).
2. Ø. Midtgaard, R.E. Hansen, P.E. Hagen and N. Størkersen. *Imaging sensors for autonomous underwater vehicles in military operations*. Proc.SET-169 Military Sensors Symposium. Friedrichshafen, Germany. (May 2011).
3. M. Harris, W. Avera, C. Steed et al. *AQS-20 through-the-sensor (TTS) performance assessment*. Proc.MTS/IEEE Oceans'05 Conf. Washington DC, USA. (Sep 2005).
4. V. Myers, G. Davies, Y. Petillot and S. Reed. *Planning and evaluation of AUV missions using data-driven approaches*. Proc.MINWARA Conference. Monterey, CA, USA. (May 2006).

5. S. Reed, Y. Petillot and A. Cormack. *PATT: a performance analysis and training tool for the assessment and adaptive planning of mine counter measures (MCM) operations*. Proc.Institute of Acoustics. Vol. 29 (6). 19-28. (Sep 2007).
6. J. Gazagnaire, P. Beaujean and J. Stack. *Combining model-based and in situ performance prediction to evaluate detection & classification performance*. Proc.Institute of Acoustics. Vol. 29 (6). 11-18. (Sep 2007).
7. Ø. Midtgaard, T.O. Sæbø and R.E. Hansen. *Estimation of detection / classification performance using interferometric sonar coherence*. Proc.3rd international Conference on Underwater Acoustic Measurements (UAM). 335-342. Nafplion, Greece. (Jun 2009).
8. R.E. Hansen and T.O. Sæbø. *Towards Automated Performance Assessment in Synthetic Aperture Sonar*. Proc.MTS/IEEE Oceans Europe. Bergen, Norway. (Jun 2013).
9. M. Geilhufe and Ø. Midtgaard. *Quantifying the complexity in sonar images for MCM performance estimation*. Proc.2nd Underwater Acoustics Conference. 1041-1048. Rhodes, Greece. (Jun 2014).
10. P.E. Hagen, T.G. Fossum and R.E. Hansen. *HISAS 1030: The next generation mine hunting sonar for AUVs*. Proceedings of UDT Pacific 2008 Conference. Sydney, Australia. (Nov 2008).
11. G. Franceschetti and R. Lanari. *Synthetic Aperture Radar Processing*. CRC Press, (1999).
12. C. Oliver and S. Quegan. *Understanding Synthetic Aperture Radar Images*. SciTech Publishing, Inc., Raleigh, NC, (2004).
13. J.C.V. Jakowatz, D.E. Wahl, P.H. Eichel, D.C. Ghiglia and P.A. Thompson. *Spotlight-Mode Synthetic Aperture Radar: A Signal Processing Approach*. Kluwer Academic Publishers, (1996).
14. D.A. Cook and D.C. Brown., '*Analysis of Phase Error Effects on Stripmap SAS*', IEEE Journal of Oceanic Engineering 34 (3) 250-262. (2009).
15. D. Massonnet and J.C. Souyris. *Imaging with synthetic aperture radar*. EFPL Press, (2008).
16. X. Lurton. *An Introduction to Underwater Acoustics: Principles and Applications*. Springer Praxis Publishing, (2010).
17. T.O. Sæbø. *Seafloor Depth Estimation by means of Interferometric Synthetic Aperture Sonar* [PhD thesis]. University of Tromsø, Norway. (2010).
18. M. Pinto., '*High Resolution Seafloor Imaging with Synthetic Aperture Sonar*', IEEE Oceanic Eng.Newsletter. 15-20. (2002).
19. S.A. Synnes, R.E. Hansen and T.O. Sæbø. *Assessment of shallow water performance using interferometric sonar coherence*. Proc.3rd international Conference on Underwater Acoustic Measurements (UAM). 1391-1396. Nafplion, Greece. (Jun 2009).
20. O. Daniell, Y. Petillot and S. Reed. *Unsupervised Sea-Floor Classification for Automatic Target Recognition*. Proc.International Conference on Underwater Remote Sensing. Brest, France. (Oct 2012).
21. R.E. Hansen, A.P. Lyons, T.O. Sæbø, H.J. Callow, and D.A. Cook., '*The effect of internal wave-related features on synthetic aperture sonar*', IEEE Journal of Oceanic Engineering (In press) (2014).
22. M. Geilhufe. *Statistical Analysis of Lattice Data with Wavelet Variance Methods and Spatiotemporal Modeling of Infectious Disease Spread* [PhD thesis]. University of Tromsø, Norway. (2013).
23. D.B. Percival and A.T. Walden. *Wavelet methods for time series analysis*. Cambridge University Press, (2000).
24. V. Myers and M. Pinto., '*Bounding the performance of sidescan automatic target recognition algorithms using information theory*', IET Radar, Sonar & Navigation. Vol 1(4). 266-273. (2007).
25. M. Couillard, S. Dugelay, A. Grati et al. *MANEX'13: summary and preliminary results*. NATO STO-CMRE, CMRE-MR-2014-001. La Spezia, Italy. (2014).